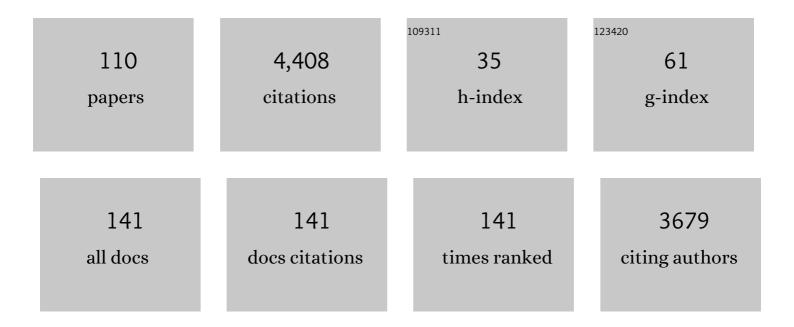
List of Publications by Year in descending order

Source: https://exaly.com/author-pdf/9563924/publications.pdf Version: 2024-02-01



#	Article	IF	CITATIONS
1	Temporal and spatial resolution of rainfall measurements required for urban hydrology. Journal of Hydrology, 2004, 299, 166-179.	5.4	347
2	HyMeX-SOP1: The Field Campaign Dedicated to Heavy Precipitation and Flash Flooding in the Northwestern Mediterranean. Bulletin of the American Meteorological Society, 2014, 95, 1083-1100.	3.3	262
3	Radar for hydrology: Unfulfilled promise or unrecognized potential?. Advances in Water Resources, 2013, 51, 357-366.	3.8	207
4	Experimental Quantification of the Sampling Uncertainty Associated with Measurements from PARSIVEL Disdrometers. Journal of Hydrometeorology, 2011, 12, 352-370.	1.9	144
5	Multiregional Satellite Precipitation Products Evaluation over Complex Terrain. Journal of Hydrometeorology, 2016, 17, 1817-1836.	1.9	123
6	The importance of hydraulic groundwater theory in catchment hydrology: The legacy of Wilfried Brutsaert and Jean-Yves Parlange. Water Resources Research, 2013, 49, 5099-5116.	4.2	114
7	Monitoring and prediction in early warning systems for rapid mass movements. Natural Hazards and Earth System Sciences, 2015, 15, 905-917.	3.6	107
8	Improved interpolation of meteorological forcings for hydrologic applications in a Swiss Alpine region. Journal of Hydrology, 2011, 401, 77-89.	5.4	101
9	Identification of Dry and Rainy Periods Using Telecommunication Microwave Links. IEEE Geoscience and Remote Sensing Letters, 2010, 7, 611-615.	3.1	90
10	Quantification and Modeling of Wet-Antenna Attenuation for Commercial Microwave Links. IEEE Geoscience and Remote Sensing Letters, 2013, 10, 1195-1199.	3.1	90
11	Orographic effects on snow deposition patterns in mountainous terrain. Journal of Geophysical Research D: Atmospheres, 2014, 119, 1419-1439.	3.3	84
12	Correction of raindrop size distributions measured by Parsivel disdrometers, using a two-dimensional video disdrometer as a reference. Atmospheric Measurement Techniques, 2015, 8, 343-365.	3.1	83
13	High-Resolution Vertical Profiles of X-Band Polarimetric Radar Observables during Snowfall in the Swiss Alps. Journal of Applied Meteorology and Climatology, 2013, 52, 378-394.	1.5	82
14	Similarity analysis of subsurface flow response of hillslopes with complex geometry. Water Resources Research, 2005, 41, .	4.2	78
15	Path-averaged rainfall estimation using microwave links: Uncertainty due to spatial rainfall variability. Geophysical Research Letters, 2007, 34, .	4.0	76
16	Evaluation of GPM-era Global Satellite Precipitation Products over Multiple Complex Terrain Regions. Remote Sensing, 2019, 11, 2936.	4.0	74
17	Katabatic winds diminish precipitation contribution to the Antarctic ice mass balance. Proceedings of the United States of America, 2017, 114, 10858-10863.	7.1	72
18	A network of disdrometers to quantify the smallâ€scale variability of the raindrop size distribution. Water Resources Research, 2011, 47, .	4.2	71

#	Article	IF	CITATIONS
19	Hydrometeor classification through statistical clustering of polarimetric radar measurements: a semi-supervised approach. Atmospheric Measurement Techniques, 2016, 9, 4425-4445.	3.1	65
20	Influence of small scale rainfall variability on standard comparison tools between radar and rain gauge data. Atmospheric Research, 2014, 138, 125-138.	4.1	64
21	A Comparison between the GPM Dual-Frequency Precipitation Radar and Ground-Based Radar Precipitation Rate Estimates in the Swiss Alps and Plateau. Journal of Hydrometeorology, 2017, 18, 1247-1269.	1.9	64
22	Quantification of the Small-Scale Spatial Structure of the Raindrop Size Distribution from a Network of Disdrometers. Journal of Applied Meteorology and Climatology, 2012, 51, 941-953.	1.5	62
23	Solid hydrometeor classification and riming degree estimation from pictures collected with a Multi-Angle Snowflake Camera. Atmospheric Measurement Techniques, 2017, 10, 1335-1357.	3.1	62
24	Measurements of precipitation in Dumont d'Urville, Adélie Land,ÂEastÂAntarctica. Cryosphere, 2017, 11, 1797-1811.	3.9	60
25	Seasonal smallâ€scale spatial variability in alpine snowfall and snow accumulation. Water Resources Research, 2013, 49, 1446-1457.	4.2	59
26	Stochastic Super-Resolution for Downscaling Time-Evolving Atmospheric Fields With a Generative Adversarial Network. IEEE Transactions on Geoscience and Remote Sensing, 2021, 59, 7211-7223.	6.3	52
27	Hydrometeor classification from polarimetric radar measurements: a clustering approach. Atmospheric Measurement Techniques, 2015, 8, 149-170.	3.1	51
28	Detection and characterization of the melting layer based on polarimetric radar scans. Quarterly Journal of the Royal Meteorological Society, 2016, 142, 108-124.	2.7	49
29	Using Markov switching models to infer dry and rainy periods from telecommunication microwave link signals. Atmospheric Measurement Techniques, 2012, 5, 1847-1859.	3.1	47
30	Errors and Uncertainties in Microwave Link Rainfall Estimation Explored Using Drop Size Measurements and High-Resolution Radar Data. Journal of Hydrometeorology, 2010, 11, 1330-1344.	1.9	45
31	A Variational Approach to Retrieve Rain Rate by Combining Information from Rain Gauges, Radars, and Microwave Links. Journal of Hydrometeorology, 2013, 14, 1897-1909.	1.9	41
32	Polarimetric radar and in situ observations of riming and snowfall microphysics during CLACE 2014. Atmospheric Chemistry and Physics, 2015, 15, 13787-13802.	4.9	41
33	Hydrometeor classification from two-dimensional video disdrometer data. Atmospheric Measurement Techniques, 2014, 7, 2869-2882.	3.1	37
34	A radar-based regional extreme rainfall analysis to derive the thresholds for a novel automatic alert system in Switzerland. Hydrology and Earth System Sciences, 2016, 20, 2317-2332.	4.9	37
35	Evaluation of the CloudSat surface snowfall product over Antarctica using ground-based precipitation radars. Cryosphere, 2018, 12, 3775-3789.	3.9	37
36	On the fine vertical structure of the low troposphere over the coastal margins of East Antarctica. Atmospheric Chemistry and Physics, 2019, 19, 4659-4683.	4.9	37

#	Article	IF	CITATIONS
37	An Extended Kalman Filter Framework for Polarimetric X-Band Weather Radar Data Processing. Journal of Atmospheric and Oceanic Technology, 2012, 29, 711-730.	1.3	36
38	Stochastic simulation experiment to assess radar rainfall retrieval uncertainties associated with attenuation and its correction. Hydrology and Earth System Sciences, 2008, 12, 587-601.	4.9	35
39	Influence of the Subgrid Variability of the Raindrop Size Distribution on Radar Rainfall Estimators. Journal of Applied Meteorology and Climatology, 2012, 51, 780-785.	1.5	33
40	Measurement of Precipitation in the Alps Using Dual-Polarization C-Band Ground-Based Radars, the GPM Spaceborne Ku-Band Radar, and Rain Gauges. Remote Sensing, 2017, 9, 1147.	4.0	33
41	Present and Future of Rainfall in Antarctica. Geophysical Research Letters, 2021, 48, e2020GL092281.	4.0	33
42	Polarimetric Weather Radar Retrieval of Raindrop Size Distribution by Means of a Regularized Artificial Neural Network. IEEE Transactions on Geoscience and Remote Sensing, 2006, 44, 3262-3275.	6.3	32
43	Quality control of rain gauge measurements using telecommunication microwave links. Journal of Hydrology, 2013, 492, 15-23.	5.4	32
44	Spatial variability in snow precipitation and accumulation in COSMO–WRF simulations and radar estimations over complex terrain. Cryosphere, 2018, 12, 3137-3160.	3.9	32
45	Unraveling hydrometeor mixtures in polarimetric radar measurements. Atmospheric Measurement Techniques, 2018, 11, 4847-4866.	3.1	30
46	Statistical analysis of rainfall intermittency at small spatial and temporal scales. Geophysical Research Letters, 2011, 38, n/a-n/a.	4.0	29
47	Secondary ice production in summer clouds over the Antarctic coast: an underappreciated process in atmospheric models. Atmospheric Chemistry and Physics, 2021, 21, 755-771.	4.9	29
48	A stochastic model of range profiles of raindrop size distributions: Application to radar attenuation correction. Geophysical Research Letters, 2005, 32, .	4.0	28
49	Variability of the spatial structure of intense Mediterranean precipitation. Advances in Water Resources, 2009, 32, 1031-1042.	3.8	28
50	Improved Estimation of the Specific Differential Phase Shift Using a Compilation of Kalman Filter Ensembles. IEEE Transactions on Geoscience and Remote Sensing, 2014, 52, 5137-5149.	6.3	27
51	RainForest: a random forest algorithm for quantitative precipitation estimation over Switzerland. Atmospheric Measurement Techniques, 2021, 14, 3169-3193.	3.1	27
52	Microphysics and dynamics of snowfall associated with a warm conveyor belt over Korea. Atmospheric Chemistry and Physics, 2020, 20, 7373-7392.	4.9	26
53	A preliminary investigation of radar rainfall estimation in the Ardennes region and a first hydrological application for the Ourthe catchment. Natural Hazards and Earth System Sciences, 2005, 5, 267-274.	3.6	24
54	Stochastic Simulation of Intermittent DSD Fields in Time. Journal of Hydrometeorology, 2012, 13, 621-637.	1.9	24

#	Article	IF	CITATIONS
55	Retrieval of the raindrop size distribution from polarimetric radar data using double-moment normalisation. Atmospheric Measurement Techniques, 2017, 10, 2573-2594.	3.1	24
56	Influence of the Vertical Profile of Reflectivity on Radar-Estimated Rain Rates at Short Time Steps. Journal of Hydrometeorology, 2004, 5, 296-310.	1.9	22
57	Stochastic simulation of intermittent rainfall using the concept of "dry drift― Water Resources Research, 2014, 50, 2329-2349.	4.2	22
58	Nonstationarity in Intermittent Rainfall: The "Dry Drift― Journal of Hydrometeorology, 2014, 15, 1189-1204.	1.9	22
59	Multifrequency Radar Observations Collected in Southern France during HyMeX-SOP1. Bulletin of the American Meteorological Society, 2015, 96, 267-282.	3.3	22
60	Microphysics of Snowfall Over Coastal East Antarctica Simulated by Polar WRF and Observed by Radar. Journal of Geophysical Research D: Atmospheres, 2019, 124, 11452-11476.	3.3	22
61	Reconstructing the Drizzle Mode of the Raindrop Size Distribution Using Double-Moment Normalization. Journal of Applied Meteorology and Climatology, 2019, 58, 145-164.	1.5	22
62	Quantitative analysis of X-band weather radar attenuation correction accuracy. Natural Hazards and Earth System Sciences, 2006, 6, 419-425.	3.6	20
63	The vertical structure of precipitation at two stations in East Antarctica derived from micro rain radars. Cryosphere, 2019, 13, 247-264.	3.9	20
64	Challenging and Improving the Simulation of Midâ€Level Mixedâ€Phase Clouds Over the Highâ€Latitude Southern Ocean. Journal of Geophysical Research D: Atmospheres, 2021, 126, e2020JD033490.	3.3	20
65	A high space–time resolution dataset linking meteorological forcing and hydro-sedimentary responseÂinÂa mesoscale Mediterranean catchment (Auzon) ofÂtheĂArdèche region, France. Earth System Science Data, 2017, 9, 221-249.	9.9	20
66	Geostatistical simulation of twoâ€dimensional fields of raindrop size distributions at the mesoâ€∢i>γ scale. Water Resources Research, 2009, 45, .	4.2	19
67	Summer Snowfall Workshop: Scattering Properties of Realistic Frozen Hydrometeors from Simulations and Observations, as well as Defining a New Standard for Scattering Databases. Bulletin of the American Meteorological Society, 2018, 99, ES55-ES58.	3.3	19
68	Evaluation of CloudSat snowfall rate profiles by a comparison with in situ micro-rain radar observations in East Antarctica. Cryosphere, 2019, 13, 943-954.	3.9	19
69	Small-Scale Variability of the Raindrop Size Distribution and Its Effect on Areal Rainfall Retrieval. Journal of Hydrometeorology, 2016, 17, 2077-2104.	1.9	18
70	Precipitation at Dumont d'Urville, Adélie Land, East Antarctica: the APRES3 field campaigns dataset. Earth System Science Data, 2018, 10, 1605-1612.	9.9	17
71	Synoptic conditions and atmospheric moisture pathways associated with virga and precipitation over coastal Adélie Land in Antarctica. Cryosphere, 2020, 14, 1685-1702.	3.9	17
72	Estimating the Vertical Structure of Intense Mediterranean Precipitation Using Two X-Band Weather Radar Systems. Journal of Atmospheric and Oceanic Technology, 2005, 22, 1656-1675.	1.3	16

#	Article	IF	CITATIONS
73	A Versatile Method for Ice Particle Habit Classification Using Airborne Imaging Probe Data. Journal of Geophysical Research D: Atmospheres, 2018, 123, 13,472.	3.3	16
74	From model to radar variables: a new forward polarimetric radar operator for COSMO. Atmospheric Measurement Techniques, 2018, 11, 3883-3916.	3.1	16
75	A sun-tracking method to improve the pointing accuracy of weather radar. Atmospheric Measurement Techniques, 2012, 5, 547-555.	3.1	15
76	2DVD Data Revisited: Multifractal Insights into Cuts of the Spatiotemporal Rainfall Process. Journal of Hydrometeorology, 2015, 16, 548-562.	1.9	15
77	Highâ€Resolution Simulation Study Exploring the Potential of Radars, Crowdsourced Personal Weather Stations, and Commercial Microwave Links to Monitor Smallâ€Scale Urban Rainfall. Water Resources Research, 2018, 54, 10,293.	4.2	15
78	Gravity Wave Excitation during the Coastal Transition of an Extreme Katabatic Flow in Antarctica. Journals of the Atmospheric Sciences, 2020, 77, 1295-1312.	1.7	15
79	Invariance of the Double-Moment Normalized Raindrop Size Distribution through 3D Spatial Displacement in Stratiform Rain. Journal of Applied Meteorology and Climatology, 2017, 56, 1663-1680.	1.5	14
80	Orographic Flow Influence on Precipitation During an Atmospheric River Event at Davis, Antarctica. Journal of Geophysical Research D: Atmospheres, 2022, 127, .	3.3	13
81	Rainfall rate retrieval in presence of path attenuation using C-band polarimetric weather radars. Natural Hazards and Earth System Sciences, 2006, 6, 439-450.	3.6	12
82	Accuracy of Phase-Based Algorithms for the Estimation of the Specific Differential Phase Shift Using Simulated Polarimetric Weather Radar Data. IEEE Geoscience and Remote Sensing Letters, 2014, 11, 763-767.	3.1	12
83	Quantification of the radar reflectivity sampling error in non-stationary rain using paired disdrometers. Geophysical Research Letters, 2005, 32, n/a-n/a.	4.0	11
84	Spatial interpolation of experimental raindrop size distribution spectra. Quarterly Journal of the Royal Meteorological Society, 2016, 142, 125-137.	2.7	11
85	Unsupervised classification of snowflake images using a generative adversarial network and <i>K</i> -medoids classification. Atmospheric Measurement Techniques, 2020, 13, 2949-2964.	3.1	11
86	Identification of blowing snow particles in images from a Multi-Angle Snowflake Camera. Cryosphere, 2020, 14, 367-384.	3.9	11
87	Secondary ice production processes in wintertime alpine mixed-phase clouds. Atmospheric Chemistry and Physics, 2022, 22, 1965-1988.	4.9	11
88	Radar and ground-level measurements of precipitation collected by the École Polytechnique Fédérale de Lausanne during the International Collaborative Experiments for PyeongChang 2018 Olympic and Paralympic winter games. Earth System Science Data, 2021, 13, 417-433.	9.9	10
89	On the drivers of droplet variability in alpine mixed-phase clouds. Atmospheric Chemistry and Physics, 2021, 21, 10993-11012.	4.9	10
90	Three-dimensional radiative transfer effects on airborne and ground-based trace gas remote sensing. Atmospheric Measurement Techniques, 2020, 13, 4277-4293.	3.1	10

#	Article	IF	CITATIONS
91	Variations in Snow Crystal Riming and ZDR: A Case Analysis. Journal of Applied Meteorology and Climatology, 2018, 57, 695-707.	1.5	9
92	Stochastic Space–Time Disaggregation of Rainfall into DSD fields. Journal of Hydrometeorology, 2012, 13, 1954-1969.	1.9	8
93	A year of attenuation data from a commercial dual-polarized duplex microwave link with concurrent disdrometer, rain gauge, and weather observations. Earth System Science Data, 2021, 13, 4219-4240.	9.9	8
94	Reconstruction of the mass and geometry of snowfall particles from multi-angle snowflake cameraÂ(MASC) images. Atmospheric Measurement Techniques, 2021, 14, 6851-6866.	3.1	8
95	A characterisation of Alpine mesocyclone occurrence. Weather and Climate Dynamics, 2021, 2, 1225-1244.	3.5	8
96	MASCDB, a database of images, descriptors and microphysical properties of individual snowflakes in free fall. Scientific Data, 2022, 9, 186.	5.3	8
97	Scaling analysis of the variability of the rain drop size distribution at small scale. Advances in Water Resources, 2012, 45, 2-12.	3.8	7
98	Multifractal evaluation of simulated precipitation intensities from the COSMO NWP model. Atmospheric Chemistry and Physics, 2017, 17, 14253-14273.	4.9	6
99	Integrated water vapor and liquid water path retrieval using a single-channel radiometer. Atmospheric Measurement Techniques, 2021, 14, 2749-2769.	3.1	6
100	Impact of 3D radiative transfer on airborne NO ₂ imaging remote sensing over cities with buildings. Atmospheric Measurement Techniques, 2021, 14, 6469-6482.	3.1	6
101	Dynamic Differential Reflectivity Calibration Using Vertical Profiles in Rain and Snow. Remote Sensing, 2021, 13, 8.	4.0	6
102	ERUO: a spectral processing routine for the Micro Rain Radar PRO (MRR-PRO). Atmospheric Measurement Techniques, 2022, 15, 3569-3592.	3.1	4
103	Multifractal Analysis of Snowfall Recorded Using a 2D Video Disdrometer. Journal of Hydrometeorology, 2017, 18, 2453-2468.	1.9	3
104	Objective Characterization of Rain Microphysics: Validating a Scheme Suitable for Weather and Climate Models. Journal of Hydrometeorology, 2018, 19, 929-946.	1.9	3
105	Identification of snowfall microphysical processes from Eulerian vertical gradients of polarimetric radar variables. Atmospheric Measurement Techniques, 2021, 14, 4543-4564.	3.1	3
106	Learning about the vertical structure of radar reflectivity using hydrometeor classes and neural networks in the Swiss Alps. Atmospheric Measurement Techniques, 2020, 13, 2481-2500.	3.1	3
107	R2D2: A Region-Based Recursive Doppler Dealiasing Algorithm for Operational Weather Radar. Journal of Atmospheric and Oceanic Technology, 2020, 37, 2341-2356.	1.3	3
108	Characterisation of the melting layer variability in an Alpine valley based on polarimetric X-band radar scans. Atmospheric Measurement Techniques, 2018, 11, 5181-5198.	3.1	2

#	Article	IF	CITATIONS
109	Correction of CCI cloud data over the Swiss Alps using ground-based radiation measurements. Atmospheric Measurement Techniques, 2018, 11, 4153-4170.	3.1	1
110	Simulated microphysical properties of winter storms from bulk-type microphysics schemes and their evaluation in the Weather Research and Forecasting (v4.1.3) model during the ICE-POP 2018 field campaign. Geoscientific Model Development, 2022, 15, 4529-4553.	3.6	1